Proceedings of the Pakistan Academy of Sciences:
B. Life and Environmental Sciences 53 (4): 323–335 (2016)

ISSN: 2518-4261 (print), ISSN 2518-427X (online)

Pakistan Academy of Sciences

Research Article

Catalytic Oxidation of CO and CH_4 over Hexaaluminate based Catalysts

Saad Butt

DBFZ Deutsches Biomasseforschungszentrum gemeinnützige GmbH,
TorgauerStraße 116, Leipzig 04347, Germany

Abstract: In this work, hexaaluminate based catalysts – namely $LaMnAl_{11}O_{19}$ and$Pd/LaMnAl_{11}O_{19}$ were tested for catalytic oxidation of a model gas comprising of a mixture of CO and CH_4. The co-precipitation route was employed to synthesize both catalyst sample sowing to better chances of attaining higher surface areas at higher calcination temperatures. The N_2 adsorption isotherms yielded surface areas of 20 and 14 m^2/g for $LaMnAl_{11}O_{19}$ and $Pd/LaMnAl_{11}O_{19}$ respectively. The$T_{90}$of CO (temperature at 90% conversion) were recorded at 482 °C and 185 °C for $LaMnAl_{11}O_{19}$ and $Pd/LaMnAl_{11}O_{19}$ respectively. Moreover, a methane conversion of 62 % at 700 °C was achieved over $Pd/LaMnAl_{11}O_{19}$ in comparison to only 28 % in case of $LaMnAl_{11}O_{19}$. The structural characterisation showed that a better mobility of oxygen atoms in the lattice structure of $Pd/LaMnAl_{11}O_{19}$ along with a more pronounced mass transport phenomenon yielded a better conversion of CO and CH_4 at relatively low temperatures.

Keywords: Co-precipitation, mobility, mass transport, macroporous

1. INTRODUCTION

The overwhelming awareness of environmental protection has triggered an awakening of precautionary measures to mitigate the harmful pollutants in our environment. One of the power tools which are playing a pivotal role in shielding our environment from the harmful emissions is the process of heterogeneous catalysis, and its application for post combustion of pollutants in small scale combustion systems[1]. Despite the vast spread of technologically advanced small scale combustion devices in European countries during the recent years, the old biomass combustion systems (stoves and boilers) still occupy more consumers[2]. So the need of the hour is to equip such existing as well as newly developed systems with catalysts (same concept as in automobiles) to comply with the strict threshold emission values, like in most developed countries, for instance Germany, USA, Austria etc. Against this backdrop, various catalytic materials have been studied and tested so far to mitigate the concentrations of the two harmful pollutants, out of many existing in our environment - namely carbon monoxide and methane, emitted particularly from small scale biomass combustion systems, like stoves and boilers. In this regard, there are a few potential candidates – catalysts which can beemployed to subside the concentrations of aforementioned pollutants from such systems. Such catalysts can be broadly classified in two categories: i) noble metals - Platinum Group Metals (PGM) ii) mixed metal oxides. This set of options can definitely yield promising results concerning the oxidation of carbon monoxide and methane[3].However, the economic aspect of noble metals (too expensive!!) along with their thermal instability raise questions about their application. On the other hand, the transition metal oxides are cheaper but they are renowned for their moderate activity. Such being the case, the hexaaluminates ($ABAl_{11}O_{19}$) are currently considered to be one of the substitutions for both noble metals and spinels due to their thermal stability (owing to their peculiar structure) and high oxidation activity towards hydrocarbons, like methane. However, their structural characteristics along with catalytic

Received, May 2016; Accepted, November 2016
*Email address: Saad.Butt@dbfz.de

oxidation in a model gas have to be studied before wash-coating them on a suitable support material (e.g., SiO_2, SiC, etc.) and integrating them in stoves for future experimentation.

Ersson[4] studied extensively hexaaluminates with different ion substitutions for methane, toluene and n-heptane combustion. Based on his findings, it was revealed that lanthanum based hexaaluminates used in combination with manganese ions are quite active towards methane oxidation due to the ability of the manganese ions to change their valence state from Mn^{3+} and Mn^{2+}. Moreover, in his work, palladium based hexaaluminates – $Pd/LaMnAl_{11}O_{19}$ were also tested for their oxidation activity concerningn-heptane and toluene. The results were promising in regard to catalytic oxidation of hydrocarbons over$Pd/LaMnAl_{11}0_{19}$at relatively low temperatures.

Currently, a number of synthesis routes for hexaaluminates exist like, solid state reaction, sol-gel synthesis etc., but the simplicity of the co-precipitating route along with its high surface area yield at higher calcination temperatures make the synthesis route a preference for high-temperature applications[5].Keeping the aforementioned facts into consideration, an effort has been made in this paper to scrutinize the hexaaluminates – namely $LaMnAl_{11}O_{19}$ and $Pd/LaMnAl_{11}O_{19}$ by testing both catalysts in a mixture of model gas comprising of CO and CH_4. Later on, using different characterisation techniques like N_2 - adsorption, H_2-TPR, XRD, Hg-Intrusion, an in-depth analysis has been presented to elucidate the catalytic activity of each sample based on its structural properties. In this way, the aptness of both these catalysts could be estimated for emission control in small scale combustion systems.

2. EXPERIMENTAL

2.1 Description of the Test Bench

Within the scope of this work, a catalyst test bench has been constructed which was specifically designed to test different catalysts in powder as well as in wash-coated forms (see Fig. 1).The test bench consisted of three supply points for CO, CH_4 and air. The respective concentrations of these three components could be controlled with the aid of mass flow controllers, denoted by "FC" in the Fig. 1. The self-adjusted mixture of the model gas passed through the feed-line into the inlet of the glass reactor (diameter: 1 cm; length: 130 cm). The tube furnace, holding the glass reactor, was programmed to a desired end-temperature (maximum limit of

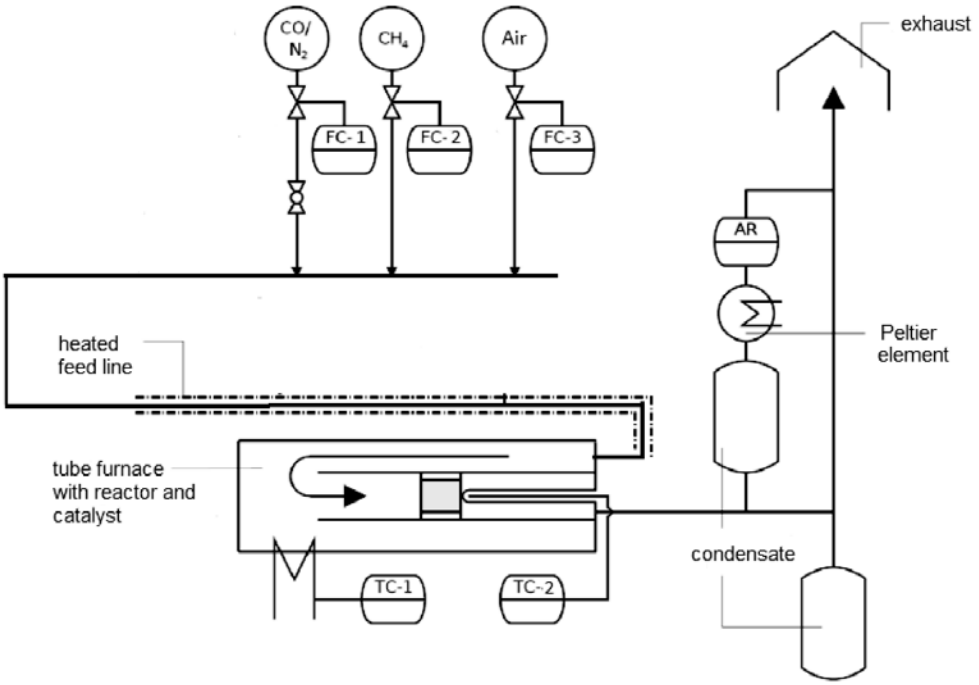

Fig. 1. The schematic layout of the catalyst test bench used for oxidation of a model gas with the aid of hexaaluminate based catalysts [6].

1100 °C) which consequently enabled the heating of the catalyst located in the glass reactor. Two pieces of quartz wool were also plugged on either side of the catalyst bed. In addition, the heating of the catalyst could be controlled with an adjustable heating rate function (K/min). The temperature of the catalyst bed was measured with a thermocouple (Type K).

2.2 Catalyst Synthesis

In this work, three catalyst samples, two based on hexaaluminates – namely, $LaMnAl_{11}O_{19}$ and $Pd/LaMnAl_{11}O_{19}$and one comprising of oxide of palladium (PdO) have been synthesized. The synthesis routes read as follows:

2.2.1. $LaMnAl_{11}O_{19}$

The nitrates of lanthanum, manganese and aluminium were dissolved in water in a stoichiometric ratio at 60 °C. The solution was acidified instantly at pH = 1 by adding HNO_3 to the solution, to avoid precipitation of Al hydroxide at this stage. The nitrate solution was then added to an ammonium carbonate solution under vigorous stirring at 60 °C. After mixing of the nitrate and carbonate solutions, instantly, the carbonates of each element were precipitated out of the solution. The slurry was aged for 2 h at 60 °C. Afterwards, the slurry was dried at 110 °C for 24 h. In the end, the sample was calcinated at 1100°C for 10 h. The catalyst was then sieved to yield particles of size in the range of 90-200 µm.

2.2.2. $Pd/LaMnAl_{11}O_{19}$

The nitrates of lanthanum, manganese, aluminium and palladium (0.6 %w/w) were dissolved in water at 60 °C. The next steps were the same as in case of $LaMnAl_{11}O_{19}$.

2.2.3. Palladium oxide-PdO

The palladium (II) nitrate dihydrate, as a precursor salt, was heated in a muffle oven at 550 °C for 3 h so that the decomposition of nitrate salt to the oxide of palladium, i.e., PdO could be ensured. The last step involved the sieving of the produced catalyst to get particles of sizein the range of 90-200 µm.

2.3 Characterisation Techniques

The characterisation of the two synthesized catalysts i.e. $LaMnAl_{11}O_{19}$ and $Pd/LaMnAl_{11}O_{19}$ was done via four techniques a) N_2-adsorption,b) XRD, c) H_2-TPR,d) Hg-Porosimetry. The N_2-adsorption for calculating the BET surface area of the two samples was carried out by using ASAP 2000 from company micromeritics where, each sample was subjected to 6 h at a temperature of liquid nitrogen (~ 77 K). The XRD patterns of both samples were obtained usingD8 Discover from Bunker AXS Karlsruhe where the measurements were made in four different frames i.e. at 15°, 35°, 60°, 75° at 2θ. Each measurement lasted for 180 s. The H_2-TPR was done with the aid of apparatus Altamira Instruments AMI-100. The reduction profiles were obtained by passing 5 % H_2/Ar flow at a rate of 0.03 l/min through the sample. The temperature was kept at 323 K for 15 min and then increased to 1273 K for 90 min at a rate of 10K/min. The amount of hydrogen consumed was measured by thermal conductivity detector (TCD) with a gain value of 50. The Hg-porosimetry was carried out by using the instrument manufactured by Thermo Scientific. The low pressure value corresponding to the pores of diameter upto 4000 nm was 400 kPa, whereas high pressure value corresponded to 400 MPa for pores upto 4 nm.

2.4 Catalytic Combustion of a Model Gas consisting of Carbon Monoxide and Methane

In order to investigate the catalytic activity of hexaaluminates – namely $LaMnAl_{11}O_{19}$ and $Pd/LaMnAl_{11}O_{19}$, the synthesized samples were loaded in powder form (particle size = 90- 200 µm) into a fixed bed quartz reactor. The composition of the model gaswas adjusted in such a way that the concentrations of carbon monoxide and methane corresponded to 1500 ng/g and 600 ng/g respectively. The concentration of oxygen was set to 13 Vol. %. Moreover, the GHSV of the feed through the catalyst bed was maintained at 77,700 hr^{-1}. The temperature of the tube furnace, containing the glass reactor was increased from 323 K to 1023 K with a heating rate of 15 K/min. The outlet of the reactor was connected to a gas analyser (Manufacturer: ABB Easy line continuous gas analyser) which enabled the measurement of

infrared active gas components like, CO_2, NO, CO, CH_4. Due to the paramagnetic behaviour of oxygen molecule, a magneto-mechanical oxygen analyser was already integrated by the manufacturer into the same infrared photometer analyser to measure oxygen concentration in the exhaust.

3. RESULTS

3.1 Catalytic Oxidation of a Model Gas consisting of CO and CH_4

For the reference purpose, the light-off curve of palladium catalyst (i.e., PdO) has been plotted in the Fig. 2 so that the catalytic activity of the hexaaluminate based catalysts could be later on compared with it. It is quite conspicuous that the palladium catalyst was found to be remarkably active towards the oxidation of both CO and CH_4, as quite renowned from previous studies [7 –11] enabling 99 % CO-conversion at nearly 160 °C with 0.16 g of sample. For methane, a T_{90} = 468 °C could be observed as shown in the Fig. 2. However, it does not come as a great surprise to witness such an astonishing catalytic activity of palladium at very low temperatures. The challenge lies in the fact that how to overcome the economic drawback of palladium metal which hinders its vast use as a catalyst in different chemical processes, and at the same time benefitting from its incredible catalytic properties. Against this backdrop, one can argue to make use of the synergetic effects of palladium in other cheaper and affordable catalysts, e.g., hexaaluminates.

In line with this, two different samples of hexaaluminates were synthesized and tested on a catalyst test bench, in a model gas stream having concentrations of CO and CH_4, corresponding to 1500 ppm and 600 ppm, respectively. The Fig. 3 shows the light-off curve of $LaMnAl_{11}O_{19}$, showing the T_{90} at 482 °C (temperature at 90 % conversion) for carbon monoxide. Moreover, a methane conversion of 28 % was recorded at T = 700 °C. The concentration of oxygen in the gas stream was always maintained at 13 Vol.%.

In order to inspect the synergetic effects of precious metals in hexaaluminates, the light-off curve of $Pd/LaMnAl_{11}O_{19}$ has been shown in theFig. 4.Clearly, there was a drastic increase in the conversion rate of both carbon monoxide as well as methane. In this regard, the T_{90} for CO could be seen at 185 °C while 62 % methane conversion was observed at T = 700 °C.

Based on catalytic activity of $Pd/LaMnAl_{11}O_{19}$

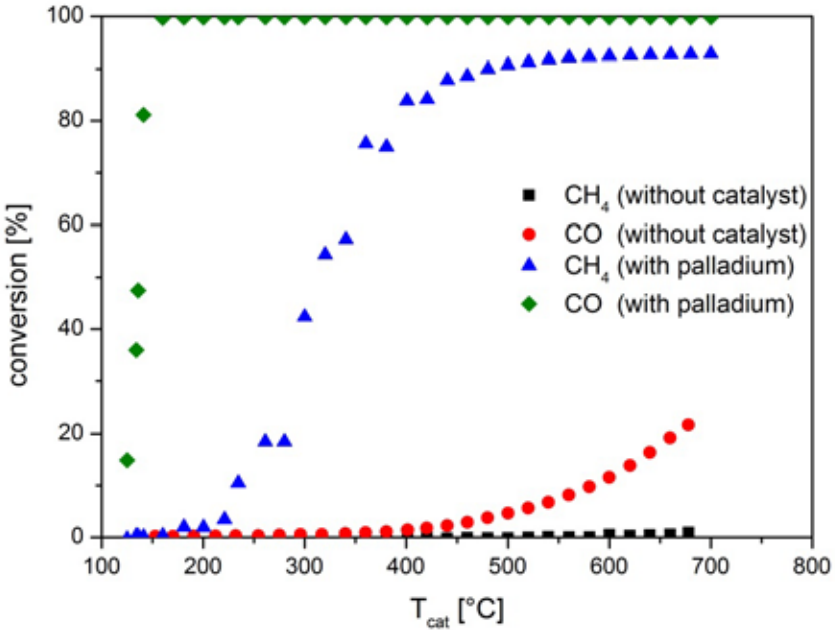

Fig. 2. The light-off curve of Pd-catalyst and its comparison with the reference experiment (without the catalyst) in the model gas mixture of CO and CH_4 (GHSV = 77,700 h^{-1}).

Table 1. An overview of the light-off temperatures of $LaMnAl_{11}O_{19}$, $Pd/LaMnAl_{11}O_{19}$ and Palladium (Pd) catalysts in the model gas feed.

Catalyst	**CO - T_{10}** [°C]	**CO-T_{90}** [°C]	**CH_4 - T_{10}** [°C]	**CH_4 -T_{30}** [°C]
Reference (without catalyst)	583	n.a.*	n.a.	n.a.
$LaMnAl_{11}O_{19}$	261	482	620	702
$Pd/LaMnAl_{11}O_{19}$	155	185	442	580
PdO	122	144	234	292

* Not achieved

(as summarized in the Table 1), one can ascertain that the combination of highly stable hexaluminates along with precious metals. e.g. *palladium* could provide the break-through needed to find a high temperature stable catalyst for total oxidation without using -Al_2O_3-washcoat with high loading of noble metals.

3.2 Catalyst Characterisation

3.2.1 BET Surface Area

The BET surface areas of the two prepared hexaaluminate samples were measured by using N_2 adsorption isotherms. The surface areas of $LaMnAl_{11}O_{19}$ and $Pd/LaMnAl_{11}O_{19}$ corresponded to $20 m^2/g$ and $14 m^2/g$ respectively.

3.2.2 XRD

The Fig. 5 depicts the XRD pattern of the sample - $LaMnAl_{11}O_{19}$. It can be observed that the XRD peaks (nearly all) corresponding to $LaMnAl_{11}O_{19}$ were shifted towards the lower angle 2θ. This shift towards the lower angles can be attributed to the tensile stress (deformation) generated within the crystal structure by irradiation of X-rays. The X-rays induce lattice distortions within a structure usually via mechanisms such as, vacancies, interstitials, replacements, local structure transformations, etc. [12].Hence, it causes the lattice parameters of a unit cell to increase (e.g., size of the unit cell) therefore, facilitating the formation of large crystallites within $LaMnAl_{11}O_{19}$ leading to peaks at

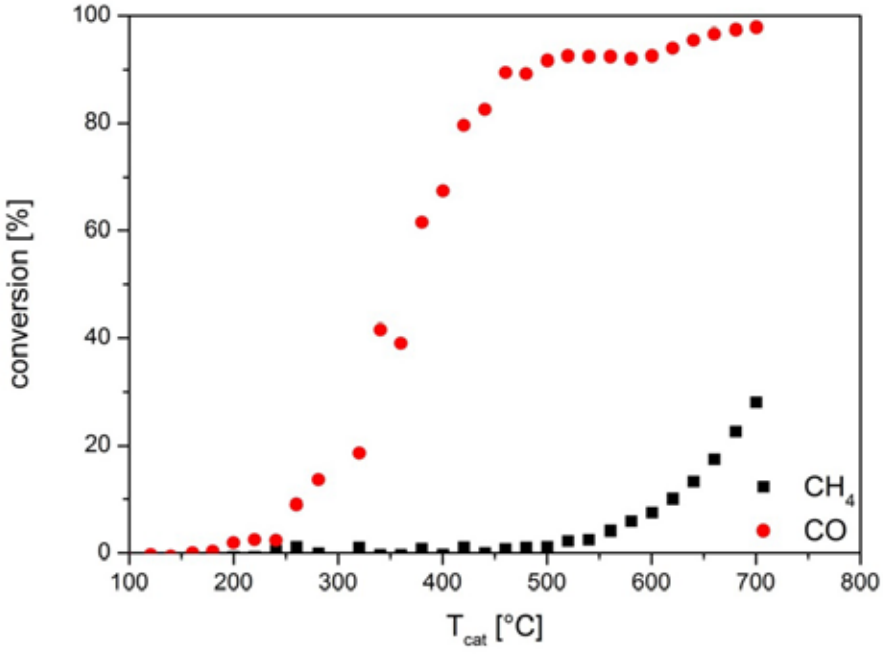

Fig. 3. The light-off curve of $LaMnAl_{11}O_{19}$ in a model gas mixture comprising of CO and CH_4 having GHSV = 77,700 h^{-1}.

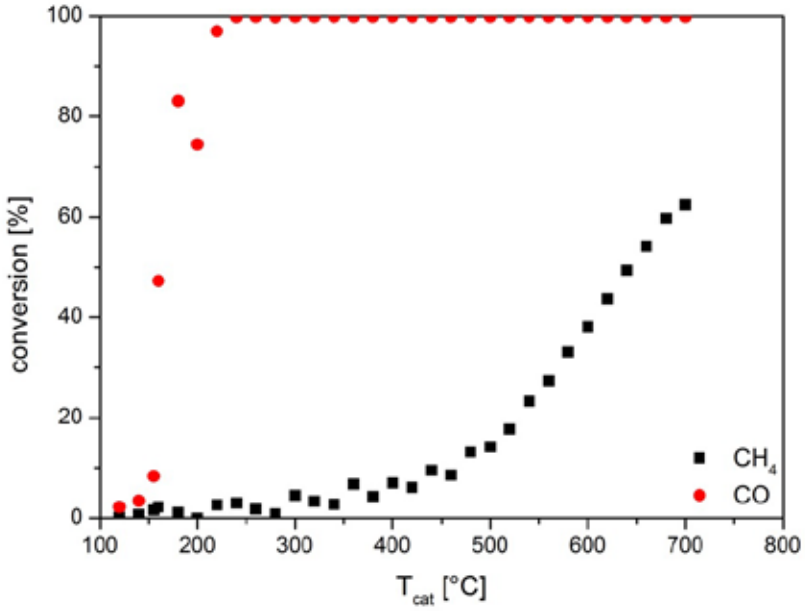

Fig. 4. The light-off curve of Pd/$LaMnAl_{11}O_{19}$ in the model gas comprising of mixture of CO and CH_4 having GHSV = 77,700 h^{-1}.

lower 2θ angles. In addition, it can be observed that the XRD pattern also contains traces of $LaAlO_3$as shown by red lines in the Fig. 5. This phase could be formed due to the lower content of manganese nitrate (precursor) in the starting solution, eventually leading to a manganese-deprived phase of aluminium lanthanum oxide on calcination at 1100 °C after co-precipitation of metal carbonates. As any XRD pattern emanates from the diffraction of the X-rays caused by the electrons in the atoms of an analysed phase, the observed higher peak intensities corresponded to the higher concentration of $LaMnAl_{11}O_{19}$. In addition, the sharp peaks in the XRD pattern can be ascribed to the presence of relatively big crystallites in the structure of $LaMnAl_{11}O_{19}$.All in all, the $LaMnAl_{11}O_{19}$ sample

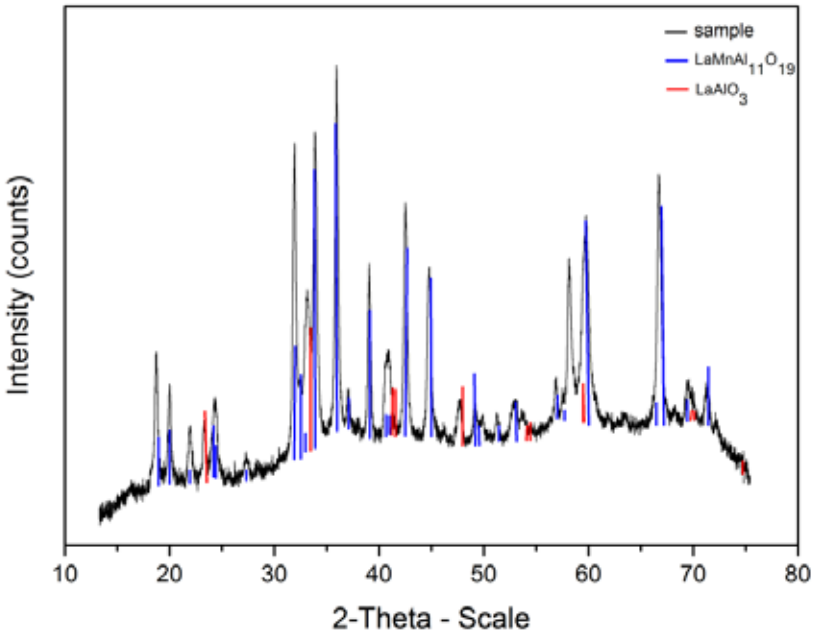

Fig. 5. The XRD pattern of the synthesized $LaMnAl_{11}O_{19}$ prepared via co-precipitation route.

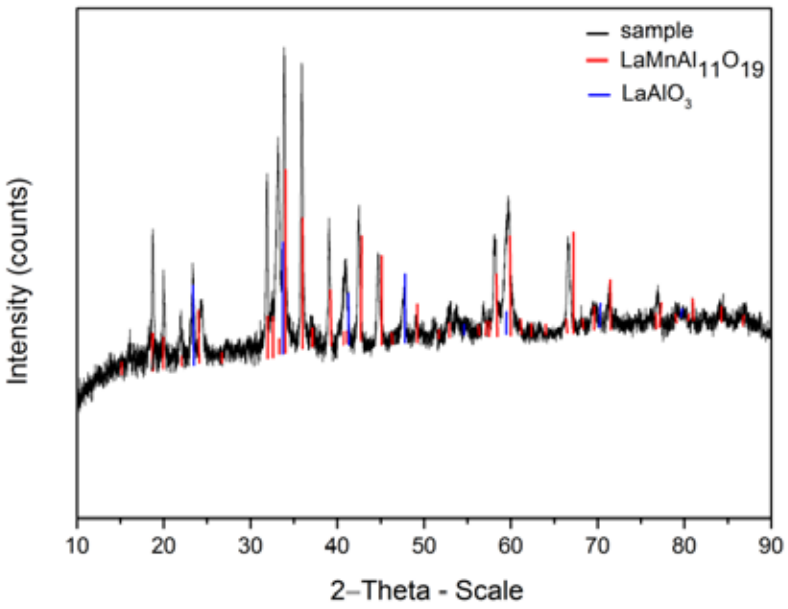

Fig. 6. The XRD pattern of the synthesized Pd/$LaMnAl_{11}O_{19}$ prepared via co-precipitation route.

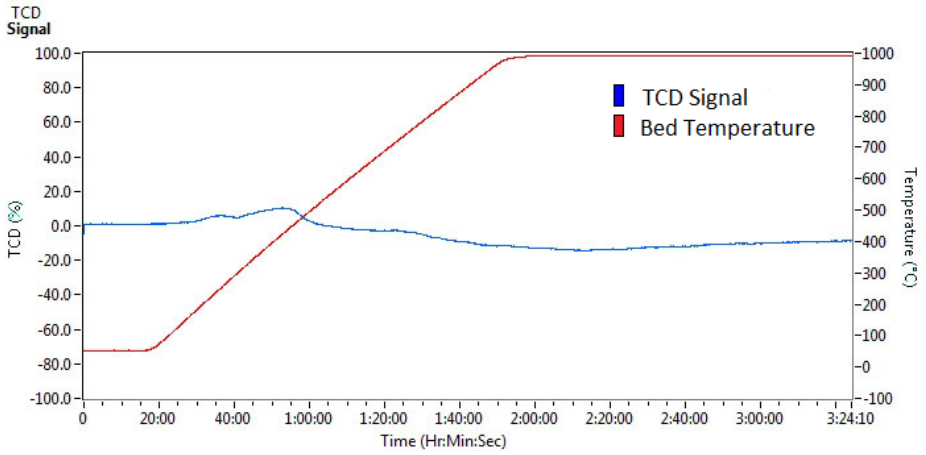

Fig. 7. H_2-TPR profile of $LaMnAl_{11}O_{19}$ synthesized using co-precipitation technique.

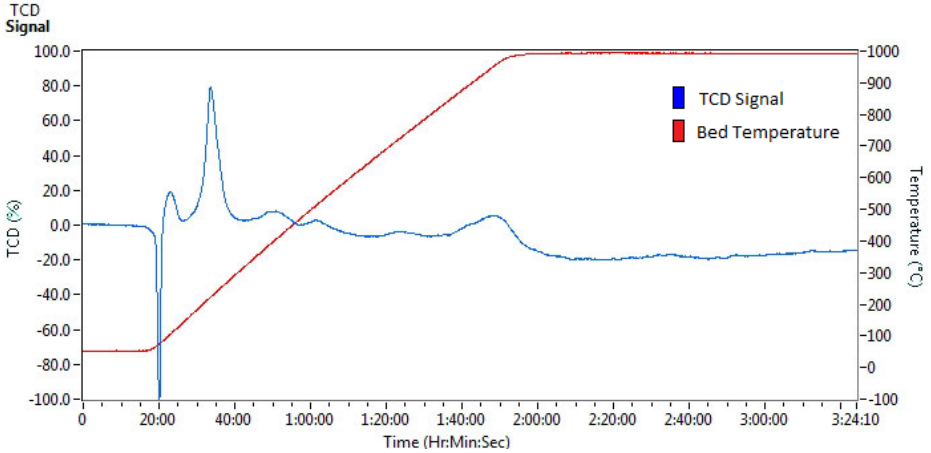

Fig. 8. H_2-TPR profile of palladium based hexaaluminate (Pd/$LaMnAl_{11}O_{19}$) synthesized via co-precipitation technique.

synthesized via co-precipitation route yielded a sample with a highly crystalline structure having bigger crystallites.

The XRD pattern of the palladium based hexaaluminate – $Pd/LaMnAl_{11}O_{19}$has been shown in the Fig. 6. It is quite evident that the XRD patterns of both catalysts i.e. $LaMnAl_{11}O_{19}$ and $Pd/LaMnAl_{11}O_{19}$were quite similar in nature. The noteworthy observation is that the XRD pattern (Fig. 6) showed no signs of palladium or any of its oxide phase (e.g., PdO) in the analysed sample. It can be due to the fact that either the PdO existed in an amorphous form or the palladium particles were so small to cause diffraction of the X-rays, and thus leading to the non-detection of palladium. Generally, the particles having a size smaller than 3 nm cannot be detected via XRD.

3.2.3 H_2-TPR

The hydrogen temperature-programmed reduction (H_2-TPR) technique has been used to determine different oxide phases and efficient reduction conditions for the synthesized $LaMnAl_{11}O_{19}$ and $Pd/LaMnAl_{11}O_{19}$ catalysts. The Fig. 7 shows the H_2-TPR profile of $LaMnAl_{11}O_{19}$. It can be seen that there exists two reduction peaks centred at around 250 °C and 400 °C, respectively. The first miniature peak corresponded to the reduction of Mn^{+3} to Mn^{+2}, whereas the second more obvious peak corresponded to the further reduction of Mn^{+2} to Mn^{+0}.

The Fig. 8 represents the H_2-TPR pattern of Pd based hexaaluminate. The negative peak at around 100 °C depicts the H_2-desoprtion initiated by decomposition of the bulk palladium hydride (PdH_X) formed through H-diffusion within the Pd crystallites [13].The second peak centred at around 120 °C could be associated to the reduction of PdO to Pd. The next two peaks at 250 °C and 400 °C, are consistent with the H_2-TPR pattern of $LaMnAl_{11}O_{19}$. Clearly, both peaks were more pronounced this time around which could be ascribed to the H_2-spillover mechanism owing to the presence of palladium in the crystal structure. The function of H_2-spillover mechanism in enhancing the hydrogen consumption of palladium based catalysts has been already reported in the literature [14]. An increase in the hydrogen adsorption and hence a better hydrogen consumption in case of Pd based hexaaluminate could be linked to spillover of hydrogen from the palladium phase on the neighbouring oxide phase of manganese. The H_2-spillover from the palladium phasetriggers the adsorption/diffusion of atomic hydrogen onto/through the neighbouring metal oxide phases, consequently enhancing the reducibility of oxide phases at 250 °C and 400 °C. Moreover, it could be seen that three additional peaks at around 520°C, 730°C and 980 °C appeared in H_2-TPR pattern of $Pd/LaMnAl_{11}O_{19}$. This additional H_2 consumption at higher temperatures could be attributed to the synergetic effects of palladium in the crystal lattice whic hyielded reaction of atomic hydrogen with various types of O^{-2} species having different mobilities [15]. In this context, the doping with palladium could have also possibly caused the reduction of $La^{+3} > La^{+2} > La^{+0}$at 520 °C and 730 °C, respectively. However, this speculation remains a speculation in this work as not so many literature references could be found on the H_2-TPR of lanthanum oxides. The last distinctive peak at around 980 °C could be attributed to the complete reduction of palladium oxide to metallic palladium [16].

3.2.4 Hg-Porosimetry

The Fig. 9 depicts the pore size distribution of the synthesized $LaMnAl_{11}O_{19}$ sample carried out using the Hg-porosimetry technique. According to IUPAC pore size classification, the synthesized catalyst pore structure can be categorized as meso- and macro-porous structure. This categorization is based on the fact that no pore size in the range of < 2 nm could be seen in the histogram, as shown in the Fig. 9. In addition, a small fraction of pores having diameter in the range between 2 -50 nm could be observed in the sample. A steep slope could be witnessed in the differential volume, i.e., dV starting from pore diameter of 50 nm which transformed into a flat slope after pore diameter of 110 nm. It leads to the fact that the analysed sample consisted primarily of the pores ranging between 50 -100 nm, i.e., macropores.

The Fig. 10 shows the pore size distribution of the palladium based hexaaluminate, i.e., $Pd/LaMnAl_{11}O_{19}$. Likewise in the case of $LaMnAl_{11}O_{19}$,

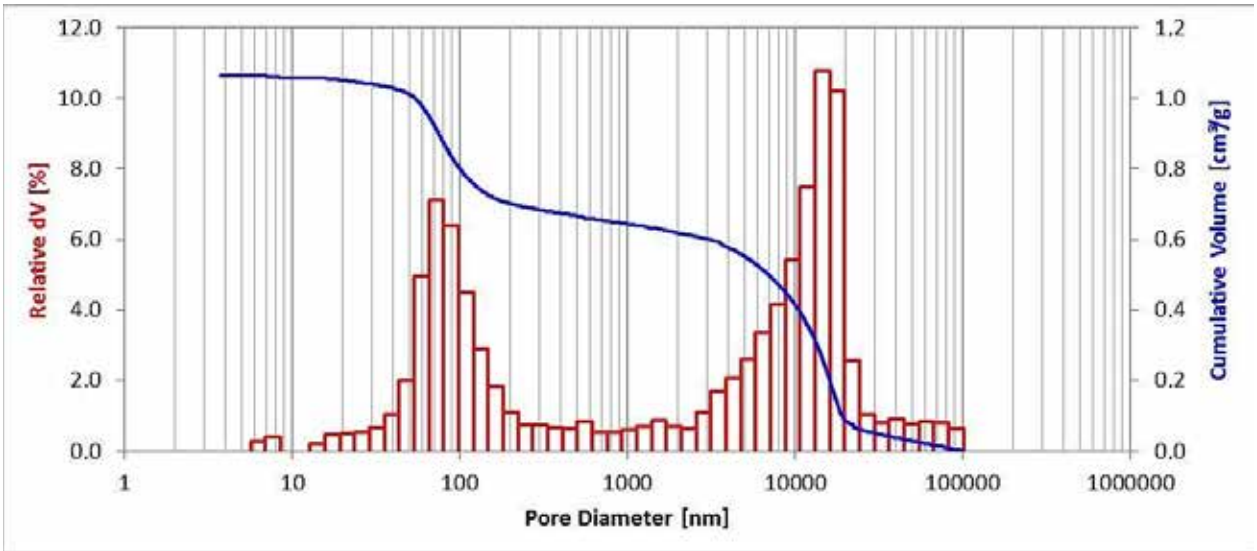

Fig. 9. Pore size distribution of $LaMnAl_{11}O_{19}$ characterized using Hg-intrusion technique.

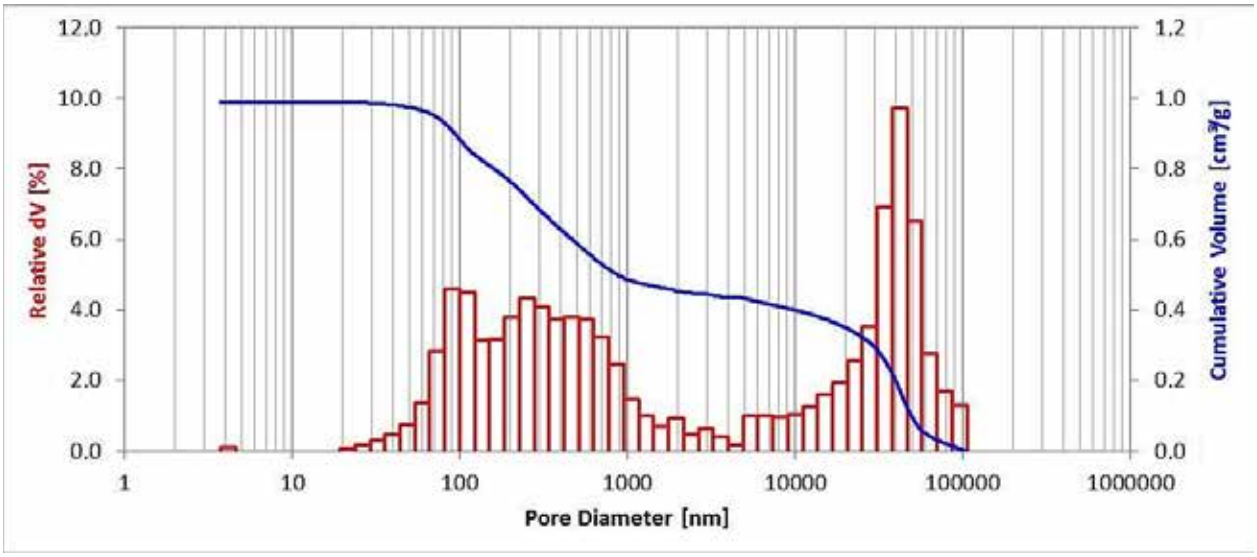

Fig. 10. Pore size distribution of $Pd/LaMnAl_{11}O_{19}$ characterized using Hg-intrusion technique.

the palladium based hexaaluminate exhibiteda macroporous structure. Clearly, there was no existence of micropores (< 2 nm) in the structure. The majority of the pores in the structure comprised of diameters in the range of 100 and 1000 nm.

4. DISCUSSION

The catalytic activities of $LaMnAl_{11}O_{19}$ and $Pd/LaMnAl_{11}O_{19}$ were examined in a model gas stream comprising of a mixture of carbon monoxide and methane, where the concentrations of both pollutants were adjusted according to the emission levels of a standard 8 kW small scale wood log stove [4].This methodology will eventually lead to make a feasibility check of the two synthesized catalysts for integration in small scale combustion systems to mitigate the harmful pollutants from such systems.

It could be seen from the light-off curves of $LaMnAl_{11}O_{19}$ and $Pd/LaMnAl_{11}O_{19}$(Fig. 3,Fig. 4) that both catalysts were quite active concerning the oxidation of the CO and CH_4. However, it was evident that the palladium based hexaaluminate, i.e., $Pd/LaMnAl_{11}O_{19}$ showed synergetic effects of palladium as the light-off temperature, in this case, was considerably lower (Table 1).The specific

surface areas (m^2/g) of both catalyst samples played a minor part in effecting the catalytic activity. As a matter of fact, the least active out of the two tested catalyst samples i.e. $LaMnAl_{11}O_{19}$ offered a higher surface area (20 m^2/g) in comparison to 14 m^2/g of Pd based hexaaluminate. It tempts to probe further the factors which could be accountable for the better activity of $Pd/LaMnAl_{11}O_{19}$. Moreover, the XRD pattern of both samples showed quite astonishing similarities as no real traces of palladium or any of its oxides could be observed in the respective pattern of $Pd/LaMnAl_{11}O_{19}$, as shown in the Fig. 6. It could be possibly due to the fact that the palladium atoms had a size smaller than 3 nm which went undetected by X-rays.

However, the first major distinctive difference between the structures of the two hexaaluminate samples, namely $LaMnAl_{11}O_{19}$ and $Pd/LaMnAl_{11}O_{19}$ could be observed in H_2-TPR profiles. The amount of hydrogen consumed in case of $LaMnAl_{11}O_{19}$ was considerably low, as could be estimated from the two relatively flat peaks, shown in the Fig. 7. It highlights the fact that the less mobility of oxygen atoms in the lattice structure of $LaMnAl_{11}O_{19}$ induced a low catalytic activity. It has been already established that the structural defects which are being produced by the dislocation of oxygen atoms in the lattice structure will enhance the catalytic activity[17]. The significance of these defects in regard to the catalytic activity is based on the fact that around these defects a variety of surface energy levels are available which may lie in the range to trigger a) electron exchange reactions between the absorbent and the lattice b) the chemical bonding of molecules and atoms with the surface [18]. In this respect, Dowden [19] has already presented his work on the facilitation of adsorption process by the structural defects.

On the other hand, the H_2-TPR profile of $Pd/LaMnAl_{11}O_{19}$ draws the attention to the fact that there exist seven reduction peaks (including the negative peak) which corresponds to an exceptional mobility of oxygen atoms in the crystal structure. In principle, this structural characteristic of $Pd/LaMnAl_{11}O_{19}$ can be attributed to the fact that palladium is quite renowned to adsorb hydrogen atoms on its surface, consequently leading to spill-over of hydrogen on neighbouring phases of oxides of manganese and lanthanum. The hydrogen spill-over stems from the phenomenon where a hydrogen molecule is first adsorbed on the palladium surface, leading to its dissociation to two hydrogen atoms, which later on diffused through the oxide phases of manganese and lanthanum[20]. As a consequence, more hydrogen can be adsorbed by palladium based hexaaluminate as compared to $LaMnAl_{11}O_{19}$. Thus, the hydrogen spill over from palladium played a pivotal in penetrating the lattice structure of $Pd/LaMnAl_{11}O_{19}$and mobilizing the oxygen atoms within the structure which ultimately brought about the reduction of manganese and lanthanum phases. Accordingly, it could be safely assumed that the molecular hydrogen produced after the catalytic oxidation of methane on active centres, supposedly, underwent molecular dissociation on the same palladium surface resulting into respective hydrogen atoms. These hydrogen atoms later diffused through the neighbouring phases and triggered the mobility of oxygen atoms within the lattice. In case of $LaMnAl_{11}O_{19}$, there was no significant surface dissociation of hydrogen molecules which eventually failed to induce the mobility of oxygen atoms within its structure. The Table 2 summarizes the energies of activation (E_a) of a methane molecule; calculated using the respective Arrhenius plots (Fig. 11), when exposed to three different catalysts. Clearly, lower activation energy of methane corresponded to its low-temperature catalytic oxidation, where PdO could be seen as a "winner" bringing down theE_a of methane to a staggering value of 30.59 kJ/mol. In short, better mobility of oxygen within the lattice structure yielded lower activation energy of methane.

Table 2. The energies of activation of methane molecule corresponding to the three tested catalysts.

Catalyst	E_a [kJ/mol]	T_{30} - CH_4
PdO	30.59	292
$Pd/LaMnAl_{11}O_{19}$	44	580
$LaMnAl_{11}O_{19}$	101	702

The pore size distribution histograms (as shown in Fig.9, 10) of both samples – $LaMnAl_{11}O_{19}$ and $Pd/LaMnAl_{11}O_{19}$ clearly manifest that the co-

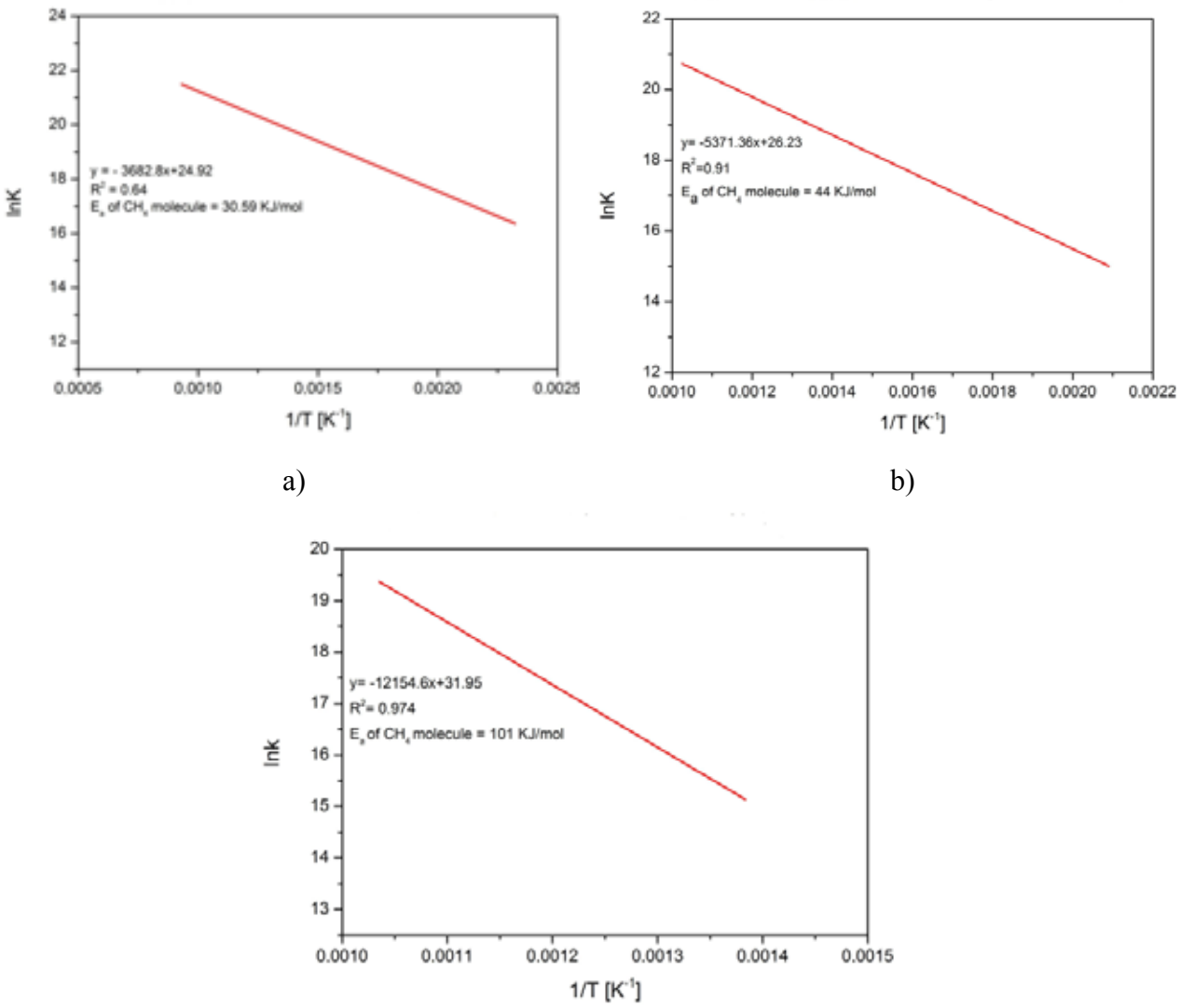

Fig. 11. The Arrhenius plots of the three synthesized catalysts for methane oxidation a) PdO b) $Pd/LaMnAl_{11}O_{19}$ c) $LaMnAl_{11}O_{19}$.

precipitation technique yielded two samples with both meso- and macro-porous structures (pore-diameter >2 nm). The underlining fact is that the majority of pores in case of$Pd/LaMnAl_{11}O_{19}$ had diameters in the range of 100 and 1000 nm, whereas the majority in $LaMnAl_{11}O_{19}$ structure comprised of diameters in the range of 50-100 nm.A catalyst structure with bigger pores definitely leads to a better mass transport of reactants through the pores but at the same time, yields a lower surface area, which can be regarded as a "trade-off". That's why, the $LaMnAl_{11}O_{19}$due to its smaller pores exhibited a larger surface area (20 m^2/g) than $Pd/LaMnAl_{11}O_{19}$ (14 m^2/g) but at the same time yielded a decline in the catalytic oxidation of CO and CH_4. To sum it all up, it can be argued that the H_2 spill over mechanism along with a better transport phenomenon in case of $Pd/LaMnAl_{11}O_{19}$ brought about a more promising catalytic oxidation of CO and CH_4 at lower temperatures.

5. CONCLUSIONS

This preliminary work investigates and elucidates the catalytic activity of hexaaluminate based catalysts – namely $LaMnAl_{11}O_{19}$ and $Pd/LaMnAl_{11}O_{19}$. The main objective behind this work was to find a suitable catalyst which could

be integrated in near-future in small scale wood stoves to mitigate the harmful pollutants from such systems. In this context, an active and economically feasible catalyst had to be first probed.

In this regard, the two catalysts were tested on a custom-made test bench where the model gas feed comprised of a mixture of CO and CH_4 with 13 Vol. %. O_2 (concentration levels referred to a standard 8 kW wood log stove). The palladium based hexaaluminate was found to be more active than $LaMnAl_{11}O_{19}$ concerning the catalytic oxidation of CO and CH_4. Based on the catalyst characterisation results, it could be argued that two factors played a pivotal role in enhancing the activity of palladium based hexaaluminate - namely a)better mobility of oxygen atoms in the lattice structure initiated by the surface adsorption and dissociation of hydrogen molecules on palladium phase; b) a more effective mass transport phenomenon in $Pd/LaMnAl_{11}O_{19}$due to bigger pore sizes (pore diameter = 10 - 1000 μm). Clearly, the pure palladium catalyst showed a higher conversion than the two hexaaluminate based catalysts. However, the synergetic effect of palladium in hexaaluminate could not be over-looked for its possible application in small scale combustions in the upcoming experiments. In line with this, a suitable support material has to be sought, onto which the hexaaluminate based catalyst, i.e., $Pd/LaMnAl_{11}O_{19}$ could be coated and later on integrated into a combustion system to validate the results presented in this work.

6. ACKNOWLEDGEMENTS

I would like to express my gratitude to "DBU – Deutsche Bundesstiftung Umwelt" for supporting and providing me with the necessary financial support.

7. REFERENCES

1. Bindig, R., S. Butt, I. Hartmann. M. Matthes, & C. Thiel. Application of heterogeneous catalysis in small-scale biomass combustion systems. *Catalysts* 2: 223–243 (2012).
2. Jokiniemi, J., K. Hytönen, J. Tissari, I. Obernberger et al. *Biomass Combustion in Residential Heating: Particulate Measurements, Sampling, and Physico-chemcial and Toxicological Characterisation*. Final Report of the Project "Biomass-PM' funded by ERA-NET Bioenergy Programme 2007–2008, University of Kuopio, Kuopio, Finland, Report 1/2008 (2008).
3. Bindig, R., S. Butt, & I. Hartmann. Application of high temperature catalysis to abate emissions from a small scale combustion system. *Agronomy Research* 12:445 – 454 (2014).
4. Ersson, A. *KTH – Kungliga Tekniska Högskolan: Materials for High Temperature Catalytic Combustion.* PhD dissertation, Stockholm University, Stockholm, Sweden (2003).
5. Groppi, G., C. Cristiani, & P. Forzatti. Preparation and characterization of hexaaluminate materials for high-temperature catalytic combustion. *Catalysis* 13: 85 –113 (1997).
6. Hermann, C. *HTWK – Hochschule für Technik, Wirtschaft und Kultur Leipzig*: *Testung von Katalysatoren für den Einsatz in Biomassekleinfeuerungsanlagen und Weiterentwicklung einer Testapparatur für die Verwendung komplexerer Modellabgas*. PhD dissertation, Leipzig University of Applied Sciences, Leipzig, Germany (2013).
7. Domingos, D., L. Rodrigues, S. Brandão. & M. Frety. Palladium-supported catalysts in methane combustion: Comparison of alumina and Zirconia supports. *Química Nova* 35: 1118–1122 (2012).
8. Shan, S., V. Petkov, L. Yang, J. Luo, et al. Atomic-structural synergy for catalytic CO oxidation over palladium–nickel nanoalloys. *Journal of the American Chemical Society* 136: 7140–7151 (2014).
9. Li, Y., Y. Yu, J. Wang, J. Song, Q. Li, M. Dong, & C. Liu. CO oxidation over graphene supported palladium catalyst. *Applied Catalysis B*: *Environmental* 125:189–196 (2012).
10. Xin, Y., H. Wang, & C. Law. Kinetics of catalytic oxidation of methane, ethane and propane overpalladium oxide. *Combustion and Flame* 161:1048 –1054 (2014).
11. Schwartz, W.R. & L.D. Pfefferle. Combustion of Methane over Palladium-Based Catalysts: Support Interactions. *Journal of Physical Chemistry C* 116: 8571– 8578 (2012).
12. Cullity, B.D. *Elements of X-Ray Diffraction*. Addison – Wesley Publishing Company, Reading, Massachusetts, p. 431– 453 (1956).
13. Cam, L., D. Thi, N. Tri. B. Thanh, D. Thi, H. Minh, & H. Si. Effect of carriers on physico-chemical properties and activity of Pdnano-catalyst in n-hexane isomerization. *Advances in Natural Sciences: Nanoscience and Nanotechnology* 4: 045001 (9 pp.) (2013).
14. Melian-Cabrera, I., M.L. Granados, & J.L. Fierro. G.Pd-modified Cu–Zn catalysts for methanol synthesis from CO_2/H_2 mixtures: catalytic structures and performance. *Journal of Catalysis* 210: 285–294 (2002).

15. Khine, M.S.S., L. Chen, S. Zhang, J. Lin, & S.P. Jiang. Syngas production by catalytic partial oxidation of methane over $(La_{0.7}A_{0.3})BO_3$ (A = Ba, Ca, Mg, Sr, and B = Cr or Fe) perovskite oxides for portable fuel cell applications. *International Journal of Hydrogen Energy* 38: 13300–13308 (2013).
16. Ozkan, U., M. Kumthekar, & G. Karakas. Characterization and temperature-programmed studies over Pd/TiO_2 catalysts for NO reduction with methane. *Catalysis Today* 40:3 –14 (1998).
17. Spendelow, J.S., Q. Xu, J.D. Goodpaster, P.J.A. Kenis, & A. Wieckowski. The role of surface defects in CO oxidation, methanol oxidation, and oxygen reduction on Pt (111). *Journal of the Electrochemical Society* 154: 238-242 (2007).
18. Garner, W.E. Adsorption and catalysis on oxides. Introductory paper. *Discussions of the Faraday Society* 8:211–215 (1950).
19. Dowden, D.A. Heterogeneous catalysis. Theoretical basis. *Journal of the Chemical Society* Part I: 242–265 (1950).
20. Mitsui, T., M.K. Rose, E. Fomin, D.F. Ogletree, & M. Salmeron. Dissociative hydrogen adsorption on palladium requires aggregates of three or more vacancies. *Nature* 422: 705 – 707(2003).